An experimental and theoretical approach for an estimation of ΔK_{th}

H. HEROLD, M. STREITENBERGER, M. ZINKE, L. ORAZI[1] and G. P. CAMMAROTA[1]

Institute of Joining and Beam Technology, Otto-von-Guericke-University Magdeburg PF4120, D-391016 Magdeburg. [1]*Institute of Metallurgy, University of Bologna, Viale Risorgimento 4, I-40136 Bologna, Italy*

Received in final form 18 January 2000

ABSTRACT The existence of a fatigue threshold value may affect the design process when a damage-tolerant design is considered that uses non-destructive techniques for evaluating the shape and dimensions of the defects inside materials. Obviously it should be possible to estimate the stress field surrounding these defects and this is not generally a problem with modern numerical methods.

Many factors are involved in determining the growth rate of a fatigue crack. Some of these are highly significant and it is possible to obtain the coefficients of a correlation function. Some others are not well defined and the only effect is to expand the scatter of experimental data.

Consider the sigmoidal curve we obtain when plotting the crack growth rate versus the applied ΔK_I. A very difficult parameter to measure but very useful for fatigue design is the ΔK_{Ith} value, because below this value a crack may be forming, hence, here ΔK_{Ith} is defined by the transition between a normal (e.g. 10^{-10} m/cycle) and a very low range of crack growth rate ($<10^{-10}$ m/cycle).

The ΔK_{Ith} value is very difficult to obtain by experimental methods because the growth rate is of the order or less than the atomic lattice span (3×10^{-10} m/cycle), but we can correlate the transition value with the cyclic crack tip plastic zone size and other structural parameters of metallic materials.

The aim of this work is to offer a contribution about the parameters which influence ΔK_{Ith} in stainless steels and welded joints based on the crack tip plastic zone radius.

Keywords fatigue threshold; stainless steel; theoretical–experimental approach; ΔK_{th}; grain size; microstructural parameters; load ratio.

THEORETICAL MODELS PRESENTED IN THE LITERATURE

It is very expensive to test for fatigue properties of materials near the threshold in terms of time and laboratory resources. For this purpose many authors have tried to develop models to correlate ΔK_{Ith} with other well-known and non-critical test properties of materials.[1] The influence of parameters, e.g. the load ratio or the environmental conditions, have been explained starting from very different physical models.

The validity range of these models is limited to particular classes of materials or application fields. Although there is difficulty when using them in engineering applications, they are very interesting as a basis for a summary of a worldwide knowledge-base on ΔK_{Ith} properties. We pay particular attention to models presented by Yoder and co-workers.[2,3] These models do not concern the conventional value of ΔK_{Ith} (the ΔK_I value when the crack growth rate falls below 10^{-10} m/cycle), but rather the 'knee' of the Paris curve. Yoder considers the knee of Fig. 1 as a physical value for the threshold when the size of the plastic zone at the crack tip equals the size of the 'microstructural control unit' for the material (e.g. austenitic grain size, a pearlitic or martensitic colony, etc.). Yoder introduced the concept of an effective grain size defined as the mean free path inside the microstructure. However, from this definition it is hard to evaluate the fatigue threshold for dual-phase alloys (e.g. duplex-steel). Also in many cases there are microstructural features at different scales (e.g. interlamellar spacing and colony dimensions in a pearlitic structure).

Correspondence: G. P. Cammarota.
E-mail: camm@bomet.fci.unibo.it

A wide discussion about the concepts of microstructural barriers at different stages of crack propagation can be found in Ref. [4].

Models detailed in the international literautre[1–14] are presented in Table 1 and are classified by the physical principles used by their authors.

Many models involve physical parameters of the materials which are very hard to obtain by an engineer during the design phase while in some instances it is impossible to bypass a fatigue threshold determination. It follows that while such models are interesting from a scientific point of view, they are not practical from an engineering standpoint.

ASTM E 647

This method concerns an operative definition of ΔK_{Ith} not considering local effects, e.g. crack closure, residual stress, crack tip blunting or branching. The threshold is defined as the asymptotic value of ΔK when the crack growth rate becomes zero. For many materials an operative definition of this value is a crack growth rate below 10^{-10} m/cycle. Nevertheless the standards suggest a definition for every material.

The experimenter has to fit, using a linear regression technique on the bilogarithmic graph $\log(\mathrm{d}a/\mathrm{d}N)$ versus $\log(\Delta K_{\mathrm{I}})$, for at least five points equally spaced between 10^{-9} and 10^{-10} m/cycle (the independent variable is the growth rate). The threshold is the intercept of this regression line with the 10^{-10} m/cycle value. When there are not so many points it is not possible to fit the last decade following specifically this procedure.

The ASTM code E 647[15] introduces the normalized K gradient defined as:

$$C = \frac{1}{K}\frac{\mathrm{d}K}{\mathrm{d}a} \tag{1}$$

It is possible to conduct a test with increasing K (C positive) and testing under a constant load in a particular situation. In this case the ΔK value constantly increases and causes the growth of the crack. These kinds of test need a very simple control system.

The other categories of test are those under a decreasing K (C negative) where the load applied continuously decreases in order to compensate for crack growth.

A maximum value for C of $-80\ \mathrm{m}^{-1}$ is suggested to avoid the influence of load history. The control program FatigueVIEW introduced by one of the authors[16] allows us to select the C coefficient so as to permit every kind of test.

Some authors propose alternative methods to determine ΔK_{Ith} with the aim to minimize the use of laboratory resources. These methods are summarized in Table 2 which cites additional references.[18,19,22]

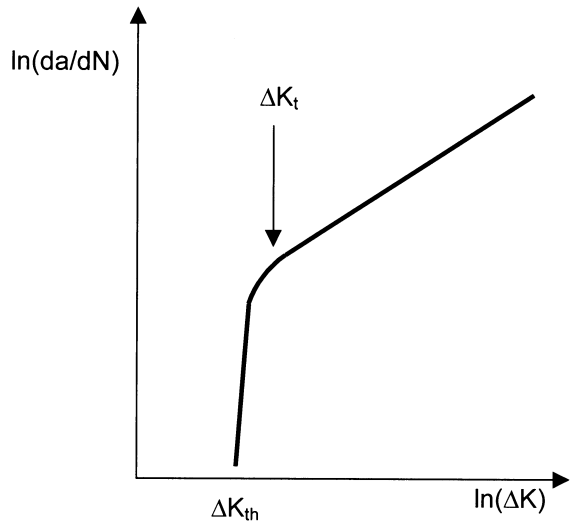

Fig. 1 The Yoder approach to fatigue threshold determination.

A THEORETICAL–EXPERIMENTAL APPROACH

A system was developed with the principal aim of conducting tests to determine ΔK_{th} by controlling the value of the C coefficient. The system is very flexible and it is able to perform virtually all kinds of fatigue tests. The starting point was a 100-kN, two-column servohydraulic test machine with an analogue control system. This system was interfaced with a personal computer, the control software FatigueVIEW (implemented in LabVIEW$^{\mathrm{TM}}$) contains a function generator that sends a signal to the feedback circuits. It is possible to vary the waveform shape, the number of digital samples and the frequency in real time.

The crack length is the most difficult parameter to measure during the fatigue propagation test. When the crack growth rate reaches values of $\sim 10^{-10}$ m/cycle, a very high precision is required. For example, if the highest possible attainable definition is only 0.01 mm then this has to be detected every 10^3 cycles.

Three experimental measuring methods were investigated: two compliance methods (on the mouth and on the specimen back face) and a direct superficial measure using crack strain gauges. The last one gives the most reliable values and was used as the reference measure. With this device it is possible to measure variation in the crack length of a few microns. The measurements were conducted following the ASTM E 647 method for decreasing the ΔK applied.

TEST MATERIALS

Two classes of stainless steel were tested. The first batch of specimens came from an AISI 304 rod, each specimen was thermally treated in order to vary the grain size. A

Table 1 Models based on dislocation theory

Sadananda and Shahinian[5]	$\Delta K_{th} = \sqrt{2\pi \cdot b} \cdot \Delta\tau$	b = Burger's vector
Yokobori and Yokobori[6]	$\Delta K_{th} = 0.38 \div 2.72 \times 10^{-5} E$	
Mutoh and Radhakrishnan[7]	$\Delta K_{th} \propto (1-R)(\sigma_y\sqrt{d}+k)\begin{cases} = \Delta K_0 + k_1\sqrt{d} \\ = \Delta K_0 + \dfrac{k_2}{\sqrt{d}} \end{cases}$	k_1 and k_2, microstructural dependent constants
Lin and Fine[8]	$\Delta K_{th} \propto q\sqrt{s}\sigma_s$	q = plasticity correction factor s = distance from dislocation σ_s = activating dislocation stress
Bartosiewicz *et al.*[9]	$\Delta K_{th} = 3.28 \cdot (1-R) \cdot \sigma_y\sqrt{d}$	
Chiang[10]	$\Delta K_{th} \propto (1-R) \cdot E \cdot \sqrt{b}\left(\sqrt{\dfrac{\rho^*}{b}} + m\sqrt{\dfrac{b}{2\pi L}}\right)$	ρ^* = root tip radius m = dislocation density L = characteristic distance from dislocation
Models based on tip plasticity		
Ravichandran[11]	$\Delta K_{th} \propto \sigma_y\sqrt{d}$	σ_y = yield strength d = grain size
Golos[12]	$\Delta K_{th} = 2\sigma_y\sqrt{\dfrac{M}{D}}\sqrt{d}$	M, D, material constants
Yoder *et al.*[2]	$\Delta K_T = 5.5\sigma_y\sqrt{d}$	For steels (this model concerns the 'knee' of Paris curve)
Purushotaman and Tien[13]	$\Delta K_{th} = \sqrt{\dfrac{a_0}{\pi\sigma_{yc}\varepsilon_p E}\ln\left(\dfrac{2}{2-(1-R)^2}\right)}$	a_0 = interatomic spacing σ_{yc} = cyclic yield strength ε_p = ductility coefficient
Models based on CTOD		
Beevers[6]	$\Delta K_{th} = \sqrt{E \cdot \Delta\sigma \cdot \mathrm{CTOD}}$	E = Young's modulus
Models based on surface energy		
Taylor[1]	$\Delta K_{th} = 2\sqrt{\dfrac{2 \cdot \gamma \cdot \pi \cdot E}{1-\nu^2-0.47 \cdot I}}$	ν = Poisson's ratio γ = surface energy I = energy function
Taylor[1]	$\Delta K_{th} = r_p\sqrt{\dfrac{2.82 \cdot \pi \cdot d}{1-\nu^2}}$	r_p = plastic zone size
Models based on environmental conditions		
Ritchie[14]	$\Delta K_{th} = f(\rho, T, \sigma_y, [\mathrm{H}], \sigma_{hyd}, \Re)$	ρ = Neuber's constant σ_{hyd} = hydrostatic stress [H] = hydrogen concentration $\Re$ = perfect gas constant T = temperature

second batch came from weld joints in AISI 2205(c) material. Synoptic tables of materials and welded joints properties are shown in Table 3.

The mean grain size was measured as another important parameter. The specimens were chemically etched to measure the grain size that followed the ASTM E112 (intercept method).[17] The results of grain size measurement and Rockwell hardness tests are shown in Table 4. The materials were machined to obtain CT specimens with a 60 mm characteristic width dimension, the thickness was 15 mm for the AISI 304 material and 5 mm for welded joints of AISI 2205(c). Each test was conducted in a laboratory environment at a load frequency of 18 Hz.

The AISI 304 material classified as 'D' is as received, while the 'A' material was annealed for 10 h at 1050 °C, the 'B' material was annealed 10 h at 1200 °C, causing a very coarse grain structure, and cooled in air causing a light sensitization.

Table 2 Alternative test methods

Authors	Assumption	Scheme	Comments
ASTM E 647[15]	$\frac{\Delta r_p}{\Delta a} = C \cdot r_p (C < 0)$ r_p = plastic zone size C = parameter	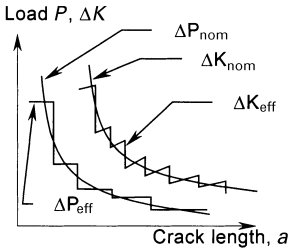	Low overload effects. Time expensive. Comparable with a lot of data in literature.
Baylon[22]	$\frac{\Delta r_p}{\Delta N} = Q \cdot r_p (Q < 0)$ N = plastic zone size Q = parameter	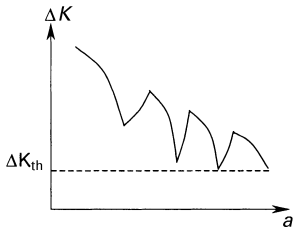	Less time consuming than above. Influenced by overload effects.
Klesnil and Lukas[18]	Decreasing steps finding successive pseudo-thresholds approaching the 'true' one	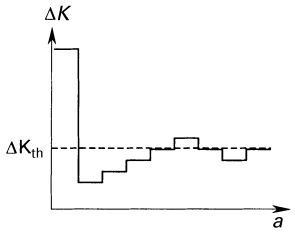	Influenced by overload effects.
Döker[22]	K_{max} = const.	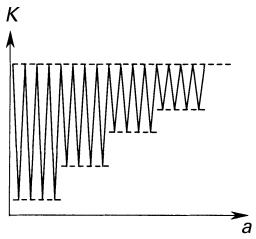	Eliminate closure effects. Not time consuming. The final R value is a dependent variable. High R values.
Pook[19]	Data obtained from S/N curves	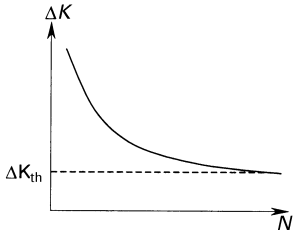	Simple test equipment. Many specimens. Useful for corrosive environments and elevated temperature studies.

THE ΔK_{th} TEST RESULTS

Some of the results are shown in Fig. 2 obtained by use of the FatigueVIEW software and following the ASTM 647/93 procedure. The tests on AISI 304 considered the effects of grain size and the load ratio when the welded specimens of AISI 2205(c) were compared with the corresponding not-welded material. The tests were conducted by shedding the applied ΔK. The Paris law coefficients were not considered because the crack path is too small compared to the plastic zone at the notch tip.

In some cases the specimens did not reach the canonical growth rate of 10^{-10} m/cycle. This was due to the limited crack gauge ligament and the very low value

Table 3 Data of the test materials (base metal and welding procedure)

Material	C	Cr	Ni	Mn	Mo	Si	P	Ti	S	Other
AISI 304	0.08	18	10.5	2.0	—	1.0	0.045	—	0.5–1.5	—
AISI 2205(c)	0.03	21 ÷ 23	4.5 ÷ 6.5	—	2.05	1.0	0.03	0.4	0.02	0.08–0.2
Filler metal										
AWS A. 5.9(b) 2209	0.03	21.5–23.5	7.5–9.5	0.5–2.0	2.5–3.5	0.9	—	—	—	—

Weld	Base material	Weld material	Welding procedure
1	AISI 2205(c)	AWS A 5.9(b) 2209	Two passes (root pass with manual GTAW and cover pass with semiautomatic pulsed GMAW)
3	AISI 2205(c)	AWS A 5.9(b) 2209	Three passes (root, inner and cover pass with manual GTAW)

Table 4 Grain size and hardness values of the test materials

AISI 304 specimens	Grain size d (μm)
A	4.4
B	25
D	2.3
AISI 2205(c)	4
Hardness HRA	
A1	52
A2	53
A3	52
A4	49
B1	52
B2	53
D1	54
D2	53
D3	53
D4	54
Weld 1	59
Weld 3	60
AISI 2205(c)	58

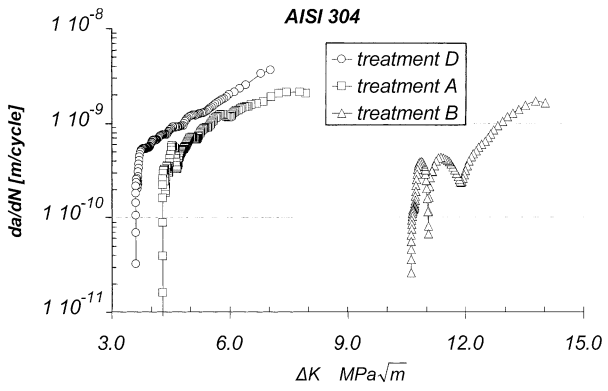

Fig. 2 Experimental ΔK curves for AISI 304 base metal. Treatment A: annealed for 10 h at 1050 °C. Treatment B: annealed for 10 h at 1200 °C. Treatment D: as received.

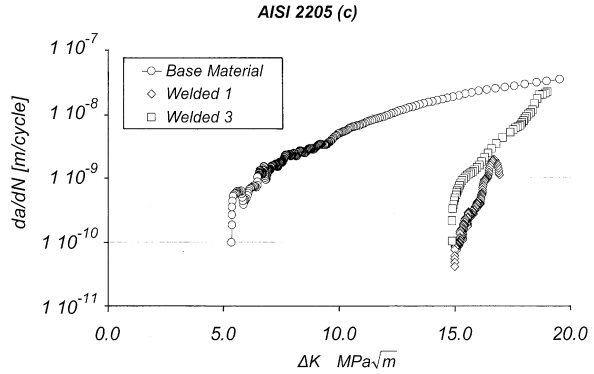

Fig. 3 Experimental ΔK curve of AISI 2205(c), base metal and both weld metals.

of the Paris exponent (∼2). These facts lead to a high crack growth before reaching a growth rate of $\sim 10^{-10}$ m/cycle. Some tests were stopped because we were no longer able to measure the crack length.

The transition between the low and high crack growth rate stage is influenced by grain size, yield strength, hardening exponent and load ratio.

Figure 2 shows the fatigue threshold results for AISI 304 classified for various treatments, which was tested at a load ratio of 0.5.

Figure 3 shows the fatigue threshold results for AISI 2205(c) base material and welded joints. The welded materials have a very high fatigue threshold. That is due to the obstacles to propagation which give a very low mean free path and localized hardening.

A THEORETICAL APPROACH

A theoretical approach was developed starting from the crack tip plasticity radius equations. This radius is given by Irwin[20] and McClintock and Irwin[21] for the plane strain condition as:

$$r_p = \frac{1}{6\pi}\left(\frac{K_I}{\sigma_y}\right)^2 \quad (2)$$

From the above equation, the Mutoh and Radhakrishnan model[7] assumes that the plastic radius is comparable to grain size and then applies two hypotheses, i.e. (i) during the nucleation phase the plastic radius is comparable to grain size; and (ii) near the crack tip there is a hardened zone. In this work, we consider a hardening coefficient, the yield stress and the tensile stress ratio.

A possible theoretical approach for the threshold could be:

$$\Delta K_{\mathrm{I,th}} = \frac{\sigma_{\mathrm{y}}\sqrt{6\pi d}}{(\sigma_{\mathrm{y}}/\sigma_{\mathrm{u}})}(1-R)^{0.3} \tag{3}$$

where σ_{u} is the tensile strength, σ_{y} is the yield stress, d is the grain size and R the load ratio. Some fatigue threshold values obtained by experiments are compared with this theoretical model in Table 5. There is a good agreement for some classes of materials having a homogeneous structure, but more problems are encountered within inhomogeneous structures, e.g. these at welded joints.

If a low value of ΔK is applied, the plastic deformation is completely included in a single grain and the grain boundary strongly affects the fatigue threshold. Many examples of these kinds of influence can be found in the literature but the data vary widely.

The test on AISI 304 stainless steel with a coarse grain obtained by a long heating treatment showed a high ΔK_{Ith} value. At the threshold the crack usually stops on a grain boundary. The ending part of the crack path is usually oriented at 45° with respect to the direction of normal stress, in some cases with a certain level of branching (Fig. 4). The crack can also be delayed or stopped by every microstructural feature, e.g. a non-metallic inclusion, and this could be a source for the dispersion of data. If the stainless steel involves carbide precipitation (sensitization) due to a low cooling rate between 450 and 900 °C, the fatigue threshold values are very high (treatment B in Fig. 2). A high sensitivity of ΔK_{Ith} to load ratio is observed in all the materials tested. This is the main difference with respect to the behaviour over the range of applicability of the Paris law. For a low load ratio the crack closure phenomenon plays a very important role.

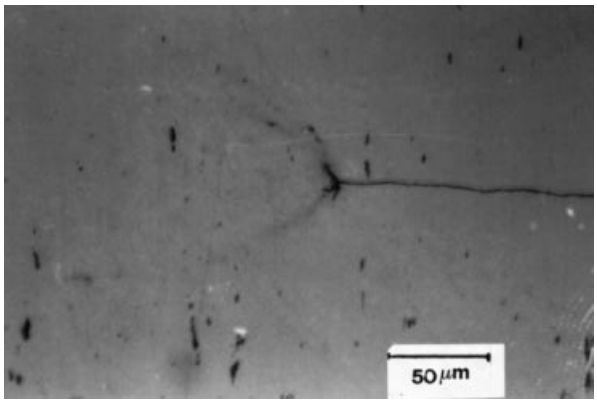

Fig. 4 The crack tip in the AISI 304.

Many models found in the literature do not match the experimental data, so a correlation, e.g. $(1-R)^{0.3}$ is proposed here, and Table 5 includes AISI 304 data for different load ratios, with a discrete agreement with the experimental data.

In conclusion, if the formulation proposed is not applicable in a general case it is confirmed that grain size, yield stress, load ratio, plane strain conditions and the hardening coefficient are the parameters mainly affecting the fatigue threshold, and it is possible to obtain good estimations of ΔK_{Ith} using these parameters.

For welded joints and the base metal of AISI 2205(c), containing the two phases of ferrite and austenite, a good agreement is achieved considering the ferrite grain size generated during the welding process.

OPTICAL METALLOGRAPHIC INVESTIGATIONS

From a macroscopic point of view, the crack surfaces are characterized by bright zones where it is possible to

Table 5 Theoretical and measured values of ΔK_{Ith}

Alloy	Load ratio	Grain size (μm)	Rs/Rm (MPa)	ΔK_{Ith} tested (MPa m$^{-0.5}$)	ΔK_{Ith} theoretical (MPa m$^{-0.5}$)
AISI 304	0.5	4.4	241/586	4.3	4.6
AISI 304	0.5	4.4	282/655	4.3	4.6
AISI 304	0.1	4.4	195/672	5.31	5.18
AISI 304	0.1	2.3	195/672	4.3	4.12
AISI 304	0.1	25	192/505	10.7	10.6
AISI 304	0.5	2.3	282/655	3.4	3.6
AISI 304	0.33	5	195/672	5.9	5.7
AISI 304	0.62	5	195/672	4.6	4.82
AISI 304	0.74	5	195/672	4.1	4.3
AISI 2205(c) base	0.1	4	405/790	6.1	6.67
AISI 2205(c) welded	0.1	17	580/760	15	14

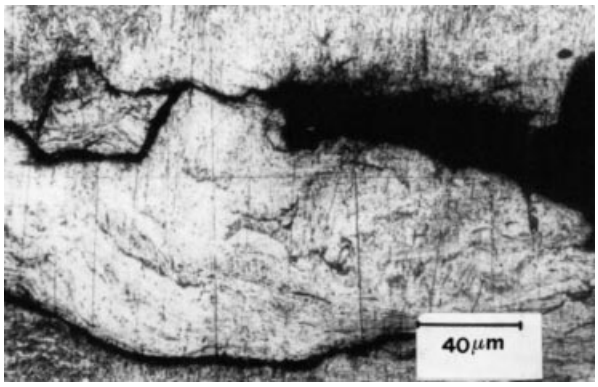

Fig. 5 A crack in welded AISI 2205(c).

observe propagation marks; usually of an arc shape. This fracture morphology is a characteristic of single-phase structures (AISI 304) corresponding to stable crack propagation. For welded joints of AISI 2205(c) the crack front is U-shaped, from which it is possible to deduce that at a low ΔK_I the crack stops propagation in plane strain zones but not in plane stress zones.

In single-phase structures the crack path is rough when the applied ΔK_I is high. An increase in roughness with increasing the grain size is found in the AISI 304 material with a very coarse grain size. In this case lateral slip planes surround the crack showing a high degree of plastic deformation.

For low values of ΔK_I, near the threshold, the crack path is quite linear (Fig. 4) and the only deviations are due to obstacles in the crack path, e.g. sulphide and oxide inclusions.

In the welded joints of AISI 2205(c), for high ΔK_I values, the crack path is irregular and frequently branched (Fig. 5). However, for low values of ΔK_I the crack path becomes regular. Due to the presence of the two phases (ferrite and austenite), the crack behaviour could be classified as 'brittle-like', but the mechanical properties of the welded joints do not indicate brittleness. In some cases the crack growth rate curve showed valleys. In these cases, when the specimen surfaces were analysed, it was possible to find defects capable of influencing the crack gauge response.

SEM INVESTIGATIONS

The SEM observations of fracture surfaces always show fatigue striations. In AISI 304 material, no differences in striation morphology were observed for high and low values of ΔK_I, in every case very fine striations were generated (Fig. 6). In AISI 2205(c), at high ΔK_I, brittle striations were observed with an irregular plate-like morphology coincident with 'quasi-cleavage' planes. These plates are widely spaced and non-continuous

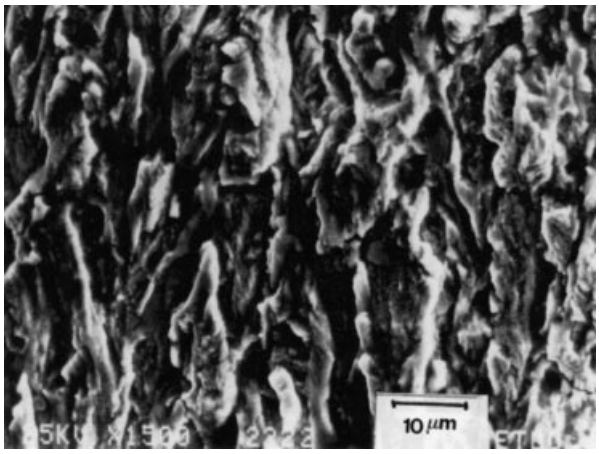

Fig. 6 The fracture surface of AISI 304.

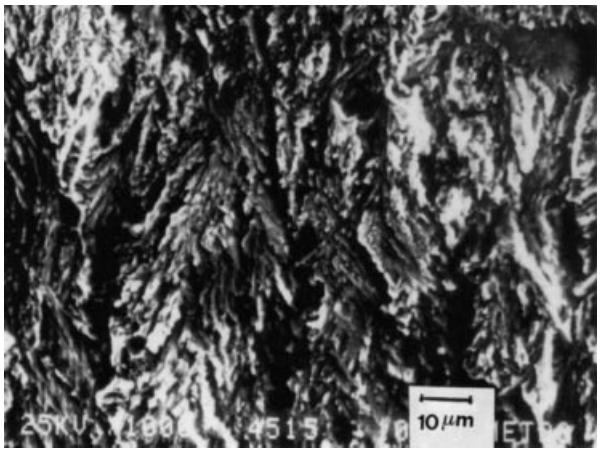

Fig. 7 The fracture surface of AISI 304 near the threshold value.

indicating a high value of plastic deformation during cycling loading. For low ΔK_I values, near the threshold of AISI 304, the main component of strain is elastic and the fatigue striations are thinner and close to one another (Fig. 7).

For welded joints, the fracture surfaces show well-defined fatigue striations with the presence of secondary cracks formed at the roots of fatigue striations [Fig. 8(a) and (b)].

SUMMARY

The decreasing ΔK_I method is the only practical method for evaluating the fatigue threshold, without introducing the influence of notch root hardening due to the machining procedures adopted when manufacturing specimens. The tests conducted with this method confirmed an increasing value of ΔK_{Ith} with increasing grain size. The grain size is the most important microstructural parameter for the steels tested here. For very coarse grain

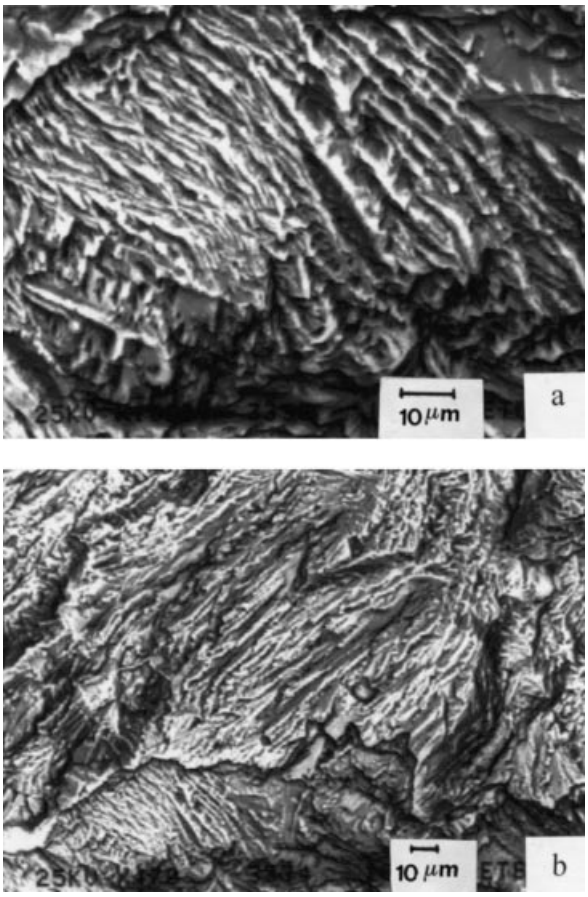

Fig. 8 Fracture surface of weld zones: (a) weld 1, AISI 2205(c); (b) weld 3, AISI 2205(c).

materials the twinning of grains should be considered when evaluating the influence of grain size on ΔK_{Ith}.

Grain boundary precipitates, as in sensitized stainless steels, or local hardening, could act as barriers for a micro-crack growing inside the grain, increasing in this manner the fatigue threshold value. Welded joints show a very high threshold value: this could be due to the welded zone morphology; the presence of many phases could act as barriers for slip lines to stop at multi-phase obstacles without generating a micro-crack.

Another important parameter experimentally verified is the load ratio. Values of R between 0.1 and 0.74 were tested. The proposed theoretical approach confirms the role of grain size, yield strength, load ratio and hardening coefficient. A calibration involving these parameters permits us to estimate the fatigue threshold. The agreement between predicted and experimental data for the tested materials is quite good.

For welded joints, in the presence of a complex multiphase microstructure, a good agreement could be achieved only by considering the primary grain size created at high temperature during the welding process.

REFERENCES

1 D. Taylor (1989) *Fatigue Thresholds*, Butterworths, UK.
2 G. R. Yoder, L. A. Cooley and T. W. Crooker (1983) A critical analysis of grain size and yield-strength dependence of near threshold fatigue crack growth in steels. *ASTM STP 791*, **1,** I-365–384.
3 G. R. Yoder, L. A. Cooley and T. W. Crooker (1982) On microstructural control of near-threshold fatigue crack growth in 7000-series aluminum alloys. *Scripta. Metall.* **16,** 1021–1025.
4 K. J. Miller (1993) Material science perspective of metal fatigue resistance. *Mater. Sci. Technol.* **9,** 453–462.
5 K. Sadananda and P. Shahinian (1977) Prediction of threshold stress intensity for fatigue crack growth using a dislocation model. *Int. J. Fracture* **13,** 585–591.
6 J. Bäklund, A. Blom and C. J. Beevers (eds) (1981) *Proc. Fatigue Thresholds*, EMAS, Warley, UK.
7 Y. Mutoh and V. M. Radhakrishnan (1981) Effect of yield stress and grain size on threshold and fatigue limit. *J. Engng Mater. Technol.* **103,** 229–233.
8 G. M. Lin and M. E. Fine (1982) Effect of grain size and cold work on the near threshold fatigue crack propagation rate and crack closure of iron. *Scripta Metall. Mater.* **16,** 1249–1254.
9 L. Bartosiewicz, L. Krause, A. Sengupta and S. K. Putatunda (1993) Application of a new model for fatigue threshold in a structural steel weldment. *Engng Fracture Mech.* **45,** 463–477.
10 C. R. Chiang (1994) Threshold stress intensity factor of fatigue cracks. *Engng Fracture Mech.* **49,** 29–33.
11 K. S. Ravichandran (1991) A rationalisation of fatigue thresholds in pearlitic steels using a theoretical model. *Acta Metall. Mater.* **39,** 1331–1341.
12 K. Golos (1988) Threshold value at low crack growth rates. In: *Proc. 8th ICSMA*, Tampere, Finland (Edited by P. O. Kettunen, T. K. Lepistö and M. Lehtonen), Pergamon Press, Oxford, UK, pp. 677–682.
13 S. Purushotaman and J. K. Tien (1978) Generalized theory of fatigue crack propagation. *Mater. Sci. Engng*, **34,** 241–246.
14 R. O. Ritchie (1977) Influence of microstructure on near-threshold fatigue-crack propagation in ultra-high strength steel. *Metal. Sci.* 368–381.
15 ASTM E 647 (1999) Standard Test Methods for Measurement of Fatigue Crack Growth Rates.
16 L. Orazi (1998) Sviluppo di un sistema completamente automatico per la conduzione di prove di fatica ed il rilievo del ΔK_{th}. In: *Acst of XXVII National Congress of Italian Association for Stress Analysis* (in Italian), pp. 953–961.
17 ASTM E 112 (1996) Standard Test Methods for Determining Average Grain Size.
18 M. Klesnil and P. Lukás (1972) Influence of strength and stress history on growth and stabilisation of fatigue crack. *Engng Fracture Mech.* **4,** 77–92.
19 L. P. Pook (1977) Practical implications of the fatigue crack growth threshold. *Metal Sci.* August/September, 382–389.
20 G. R. Irwin (1958) Fracture. In: *Encyclopedia of Physics*, Vol. VI, Springer, pp. 551–590.
21 F. A. McClintock and G. R. Irwin (1965) *ASTM STP 381*, 84.
22 A. Hadrboletz, B. Weiss and R. Stickler (1995) *Handbook of Fatigue Crack Propagation in Metallic Structures* (Edited by Andrea Carpinteri), Elsevier Science.